RSC Advances

RSC Advance

ARTICLE TYPE

Morphology control of porous epoxy resin by rod-coil block oligomer: A self-assembly induced phase separation by diphenyl fluorene modified silicone epoxy

Weixing Deng, *a,b* Yuanwei Zhong,*a* Jie Qin,*a* Xuebing Huang*a* and Jinwen Peng*a*

Self-assembly of amphiphilic rod-coil polymers into well-ordered structures has attracted significant interest over the last decade. An especially attractive application of rod-coil polymer self-assembly is the formation of porous materials. A major problem in this process is the expensive synthesis of well-defined
10 block polymers and the difficulty of up-scaling for industry applications. In this study, a robust and economical synthesis route was successfully proposed to prepare a new amphiphilic rod-coil block oligomer combining flexible silicone and rod diphenyl fluorene segment other than diblock copolymers. Porous epoxy monolith was prepared via self-assembly induced phase separation using silicone epoxy modified by diphenyl fluorene as a porogen. The morphology of the cured resin was examined by SEM
15 and the compatibility and phase separation was studied by SEM-EDS. Results showed that the pore structure of the cured epoxy monolith was controlled by the concentration of the porogen, but the average pore size kept stable. The uniform voids and particles dispersed in epoxy matrix are of the order of 1 μm or larger.

Keywords: Porous epoxy resin; self-assembly; phase separation; morphology control; rod-coil block
20 oligomer

1. Introduction

Attributable to a wide range of fascinating properties and potential applications, research interest on porous materials is continuously increasing[1-3]. Porous polymers, with the
25 advantages of low density, good thermal and electric insulation and high specific surface, have been found application in versatile fields, such as electrolysis in fuel cells[4], separation membranes[5] and tissue engineering[6]. Many methods have been developed to produce different morphologies of porous
30 polymers, such as fiber bonded nonwoven, thermally and chemically induced phase separation, freeze drying, gas foaming, porogen leaching, fused deposition modeling and electrospinning. Among these strategies, the method that associated with the use of a solvent as porogen is a robust way to manufacture porous
35 monolith, where the porous morphologies are formed due to phase separation mechanism induced in a system of polymer-solvent. However, for environmental concerns, the use of solvent and other harmful porogen should be avoided.

Amphiphilic macromolecules self-assembly into well-defined
40 supramolecular structures have attracted a lot of scientific interest over the past decades [7-10]. These ordered structures result from the balance of repulsive interactions between dissimilar segments and the conformational entropy loss of the unlike blocks. Besides, amphiphilic block copolymer self-assembly is very useful for

45 making macroporous polymers, especially materials with tailored pore size, well-defined pore architectures and long range order. Although self-assembly methodology has many merits, it has limitations. The synthesis of well defined block copolymers is often hard to scale up for expensive synthesis. From an
50 application point of view, development of simple and scalable procedures for construction of porous polymers is particularly appealing.

Epoxy resins have been widely applied in polymer industry fields as structural adhesives, coatings, encapsulation material,
55 insulating materials and composite matrix due to their superior electrical and mechanical properties, low shrinkage, good cohesiveness, excellent moisture and chemical resistance in comparison with many materials[11-15]. Thus, design of porous epoxy resins has encouraged a lot of scientific and industrial
60 efforts to realize this functional technology. In fact, porous epoxy monoliths have been produced by many groups with different methods. Kiefer[16] prepared porous epoxy by use low molecular weight liquids, Lorera[17] obtained porous epoxy by thermal oxidative degradation method and Guo[18] proceeded porous
65 epoxy by removing hyperbranched polymer. Liu[8] designed porous epoxy by the self-assembly of block copolymers. Harmful low molecular weight liquid and expensive amphiphilic block copolymer make porous epoxy difficult for wide applications. The objective of this work is to establish a general methodology

to manufacture porous cross linked epoxy with controlled porosity. The strategy is based on the self-assembly induced phase separation other than solvents as porogen. Especially, silicone epoxy modified by diphenyl fluorene was designed as the amphiphilic porogen so that silicone can provide the drive force for phase separation and diphenyl fluorene units can keep the compatibility with epoxy matrix. Furthermore, the robust synthesis of the silicone epoxy provides a practicable technique for preparing amphiphilic oligomer porogen avoiding the expensive synthesis of amphiphilic block copolymers.

2. Experimental

2.1. Materials

9,9-Bis-(4-hydroxyphenyl)-fluorene (BHPF), Dichlorodiphenylsilane (DPS), 4,4'-Diaminodiphenylsulfone (DDS), Tetrabutyl ammonium bromide (TBAB) and Epichlorohydrin (ECH) were obtained from Sigma-Aldrich. Bisphenol A epoxy resin E51 were provided by Sinopharm Chemical Reagent Co., Ltd. 1, 4-dioxane was distilled over CaH_2 under reduced pressure. Other chemical agents and organic solvents were used without further purification. All reactions were performed under a nitrogen atmosphere.

2.2. Characterization

FTIR spectra were recorded on a Nicolet Nexus 470 FTIR spectrometer in the range of 4000-500 cm^{-1}. ^{1}H-NMR characterization was carried out on a Bruker Ultra Shield Plus-400 NMR spectrometer. DSC measurements were evaluated on a NETZSCH 204C differential scanning calorimeter under a constant flow of nitrogen at 20 mL/min. The dynamic scanning experiments ranged from 25 to 350 ^{o}C at heating rates of 10 ^{o}C/min. Themogravimetric analysis (TGA) was performed on a TA Q500 thermogravimetric analyzer at a heating rate of 10 ^{o}C/min from 25 to 700 ^{o}C under a nitrogen atmosphere at a flow rate of 60 mL/min. The dynamic mechanical thermal properties of the epoxy thermosets were carried out with a TA Q800 dynamic mechanical analyzer. The samples (17.5 × 10.0 × 3.17 mm) were loaded in a single-cantilever mode at a heating rate of 3 ^{o}C/min and a frequency of 1 Hz under air atmosphere. SEM was used to study the morphology of the samples. The fracture surfaces were obtained by fracturing samples under cryogenic condition using liquid nitrogen and were examined with a Hitachi S4800 after coating with gold by vapor deposition using vacuum sputtering. Moisture absorption was determined as follow: the rectangular samples (20 × 10 × 4 mm) were dried under vacuum at 100 ^{o}C for 12 h, cooled to the ambient temperature, weighed and placed in 100 ^{o}C water for a period of time, then reweighed. The moisture absorption was calculated as the weight gain percent: moisture absorption% = $(W_t - W_o)/W_o × 100\%$, where W_t is the weight of the sample after dipping in 100 ^{o}C water for a period of time, W_o is the initial weight of the sample after placing in vacuum oven for 12 h.

2.3. Synthesis of silicone epoxy resin containing diphenyl fluorene (EGF)

7.008 g (20 mmol) 9,9-Bis-(4-hydroxyphenyl)-fluorene and 60 mL anhydrous 1,4-dioxane were added into a round bottom flask and heated to 40 ^{o}C. 2.10 mL (10 mmol) dichlorodiphenylsilane was added dropwisely to the solution. Hydrogen chloride was expelled by bubbling dry nitrogen. The reaction was stirred at 40 ^{o}C for 4 hours and heated to 70 ^{o}C followed by addition of 7.83 mL (100 mmol) ECH, 0.645 g (2 mmol) TBAB and 1.6 mL aqueous NaOH solution (50 wt %). The reaction was stirred for another 4 hours and cooled to room temperature. Excess ECH and solvent were removed and the residue was washed with water and ethanol leading to a white precipitation. Pure silicone epoxy resin containing diphenyl fluorene was obtained by recrystallization from acetone/ethanol (5:1, v/v) in 65% yield.

2.4. Preparation of the cured epoxy resin casting

Epoxy resins, E51, EGF and E51/EGF mixtures were cured with DDS. EGF was mixed with E51 in different amounts, which formed five curing systems of E51/DDS, $F_{0.1}E_{0.9}$/DDS, $F_{0.2}E_{0.8}$/DDS, $F_{0.3}E_{0.7}$/DDS, and EGF/DDS, where E and F stand for epoxy resin of E-51 and EGF, respectively.

Molten epoxy resins were completely degassed followed by addition of curing agents. Thoroughly mixed epoxy resins were casted into a preheated steel mold (220-230 ^{o}C) which was coated with mold release agent. Degasification was carefully conducted again and the mixtures were cured in their respective optimal curing condition, decided by the dynamic DSC tracing of epoxy/curing agent compositions. Cured resins were then demoulded and cut into suitable size for measurement.
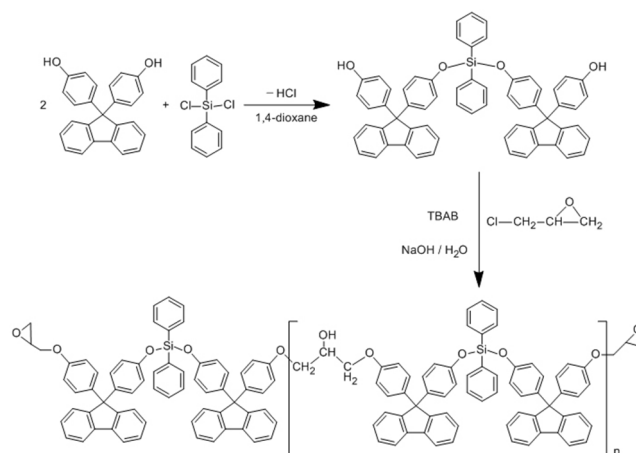
Scheme1 Synthesis routes of silicone epoxy resin containing diphenyl fluorene (EGF)

3. Results and discussion

Synthesis of EGF

Scheme 1 presents the chemical structure and the procedure for the synthesis of silicone epoxy resin containing diphenyl fluorene, which is denoted as EGF. Pure EGF was obtained by recrystallization from acetone/ethanol as white powder. The melt point of EGF is 180 ^{o}C determined by DSC.

Fig. 1 shows the ^{1}H NMR spectrum of EGF in $CDCl_3$. The chemical shifts at 7.34-7.76 are attributed to the protons on fluorene and peaks at 6.75-7.19 are attributed to the protons on phenyl groups. The characteristic chemical shifts of oxirane can be clearly read at 4.12, 3.91, 3.30 2.87 and 2.71 [19]. Fig. 2

displays the FTIR spectra of monomer BHPF and epoxy precursor EGF. The phenolic hydroxyl group absorption peak at 3481 cm^{-1} decreases because of the reaction of the OH group with epichlorohydrin [20]. The characteristic absorption peaks of
5 phenyl-oxide-silicone at 1245 cm^{-1} is evident [21] and absorption peak of oxirane at 913 cm^{-1} is clear too. In addition, the peaks located at 1034 cm^{-1} is attributed to the stretching vibrations of C-O-C, the splitting peaks at 1119 and 1111 cm^{-1} indicate the phenyl-silicone-phenyl stretching vibration, the absorption peak
10 of -CH$_2$- at 2925 cm^{-1} is observed in Fig. 2. The result of ^{1}H-NMR spectrum is in agreement with the FTIR spectrum of EGF, which further confirmed the successful synthesis of the silicone epoxy resin containing diphenyl fluorene (EGF). According to the results of the epoxy equivalent weight titration, the EEW of
15 synthesized silicone epoxy containing diphenyl fluorene EGF is 500 g / eq.
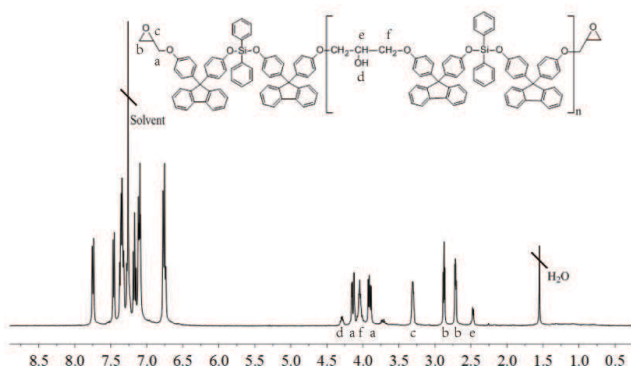
Fig. 1 ^{1}H NMR spectrum of silicone epoxy containing diphenyl fluorene (EGF) in CDCl$_3$

20
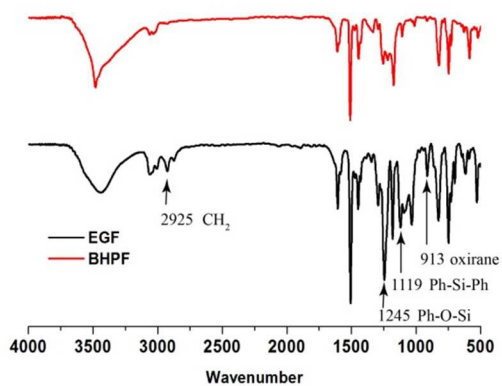
Fig. 2 FTIR spectra of BHPF and EGF oligomer

Morphologies of cured epoxy resins

Scanning electron microscopy (SEM) was used to examine the cryogenically fractured surface of the neat epoxy and EGF/E51
25 blends to reveal the texture and morphology of the phase separated system. The glassy fracture surface in the SEM photograph of the neat epoxy resin shows ripples that are due to the brittle fracture. Owing to the higher compatibility between the fluorene-epoxy blocks and the neat epoxy, the fracture surface of
30 the sample F$_{0.1}$E$_{0.9}$ (Fig. 3b) is homogeneous throughout the bulk
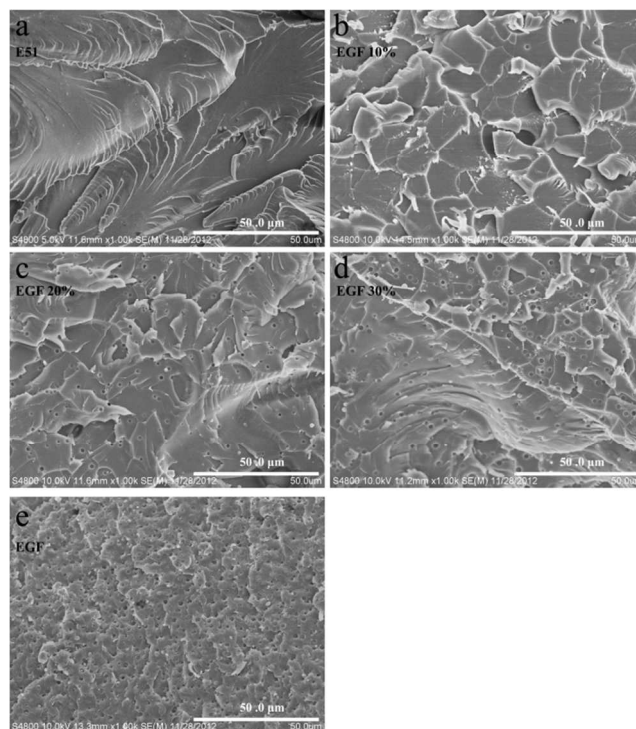
Fig. 3 SEM images of the section of cured a) neat epoxy, b) F$_{0.1}$E$_{0.9}$, c) F$_{0.2}$E$_{0.8}$, d) F$_{0.3}$E$_{0.7}$ and e) EGF. (Scale bar, 50 μm)

of the materials. However, the fractured surface has been changed
35 significantly. In the case of F$_{0.2}$E$_{0.8}$ (Fig. 3c) and F$_{0.3}$E$_{0.7}$ (Fig. 3d), the fracture surface consists of three distinct phases: globular particles and voids disperse in continuous epoxy matrix. More voids and particles were observed in cured EGF (Fig. 3e), but the morphology is still similar to that of F$_{0.2}$E$_{0.8}$ and F$_{0.3}$E$_{0.7}$. All the
40 fracture surfaces of modified epoxy networks show obvious stress whitened zone. Stress whitening is due to the scattering of visible light from the layer of the scattering centers which in this case are voids. Uniform distribution of the voids throughout the matrix is very important for toughening, as it allows the yielding process to
45 operate throughout the matrix.

For typical CTBN toughened epoxy, the fracture surface consists of dispersed particles and continuous matrix[22]. Interestingly, the fracture surface of EGF modified epoxy resin shows completely different morphologies. At low concentration of EGF
50 resin, cured epoxy resin consists of continuous matrix and a little amount of voids. With the increased inclusion of EGF resin, particles appear as the third phase dispersed in the matrix, which suggests the precipitated EGF particles in the epoxy matrix. In addition, more and more voids and particles have been developed
55 with the increased concentration of EGF resin. Despite the morphology of the cured resins has taken a dramatic change, the size of the voids and particles remain unchanged. This may result from the greater solubility of EGF resin in the epoxy. Voids and particles are of the order of 1 μm or larger. The small size of the
60 discrete particles, with a unimodal distribution, seems to indicate that phase separation started in the gelation region, so that particle growth was not possible because of the diffusion restriction existing after gelation of the epoxy matrix.
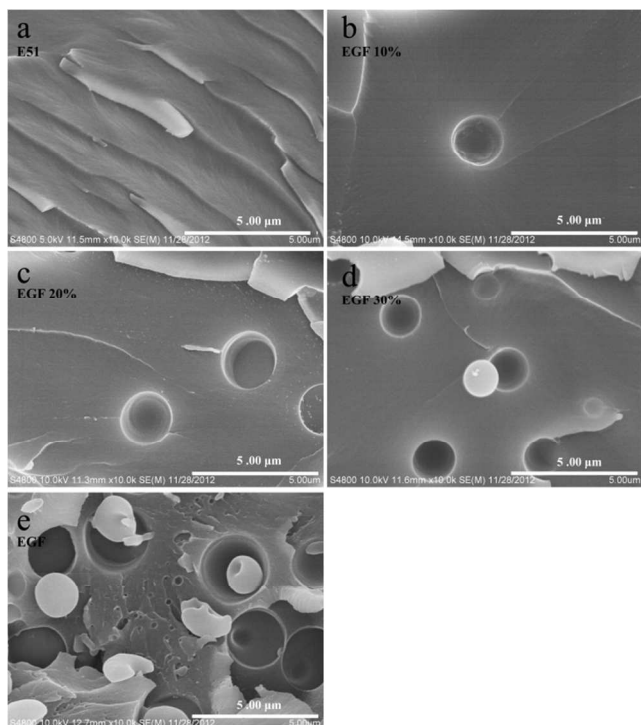
Fig. 4 SEM micrographs of fracture surface of cured epoxy resins a) E51, b) $F_{0.1}E_{0.9}$, c) $F_{0.2}E_{0.8}$, d) $F_{0.3}E_{0.7}$ and e) pure EGF resin. (Scale bar, 5 μm)

Void and particle formation model
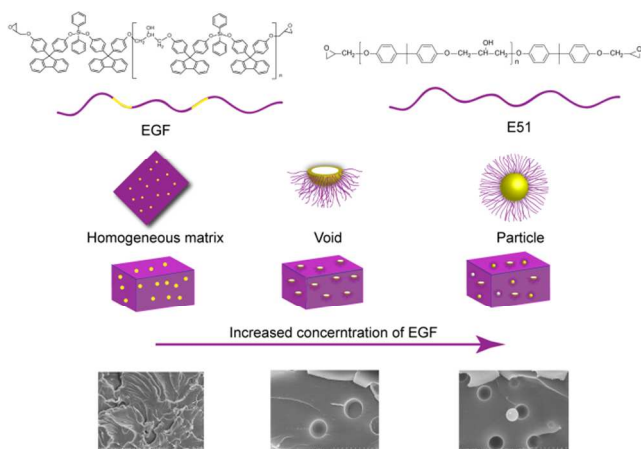
Scheme 2 Aggregation and phase separation of cure EGF/E51 resin

Si was found by EDS spectra in all cured EGF/E51 matrix and Si content in the epoxy matrix shows a weak change when the EGF resin content was improved up to 30% in the formulation (Fig. 5 a, b and c). This indicates that some amount of EGF molecules can dissolve in the epoxy matrix. In addition, the EGF shows a good compatibility with E51 at low inclusion of EGF resin (< 10% wt%), this result is agree with the morphology of the $F_{0.1}E_{0.9}$ (Fig. 3b). The compatibility should mainly be attributed to the diphenyl fluorene segment. Morphology study shows that the $F_{0.1}E_{0.9}$ sample is homogeneous throughout the bulk of the material (Fig. 3b). In fact, increased magnification shows a little amount of void in the epoxy matrix (Fig. 4b). This tendency of cured composite resin to produce more and more voids with the increased EGF content can be seen in Fig. 3 and Fig. 4. The morphology changes of cured epoxy composite resins indicate

excess inclusion of EGF resin leads to phase separation. The silicone's low surface energy and in turn the huge group of the diphenyl fluorene leads to a strong repulsive interaction between the silicone and fluorene blocks. Hence, the EGF molecules are strongly segregated and assemble into micelle with silicone groups interior for void or outer for dispersed particle. The migration and aggregation of silicone blocks were well affirmed by the EDS results (Fig. 5 d, e and f). The increase in Si in dispersed particles with the increasing EGF resin concentration indicates that the particles are composed of EGF and E51. This consists with the depression of S in dispersed particles surface (Fig. 5d, e, f). The depression in S should be attributed to the lower crosslink density since the EGF resin shows higher epoxy equivalent weight than that of E51. On the other hand, abundant Si aggregated on the surface of the particle hinders the detection of the embedded S inside of the particle. Morphology analysis and EDS spectra illustrate the mechanism and the formation process of the phase separation between the EGF resin and epoxy matrix. Three stages can be clearly found as shown in scheme 2. At the beginning, epoxy resin can accommodate small amounts of EGF (< 10% wt%) to form homogeneous phase. Then voids originate from the aggregation of excess EGF molecules. In the final stage, silicone rich particles appear as the third phase in the final morphology of this phase separation blend.
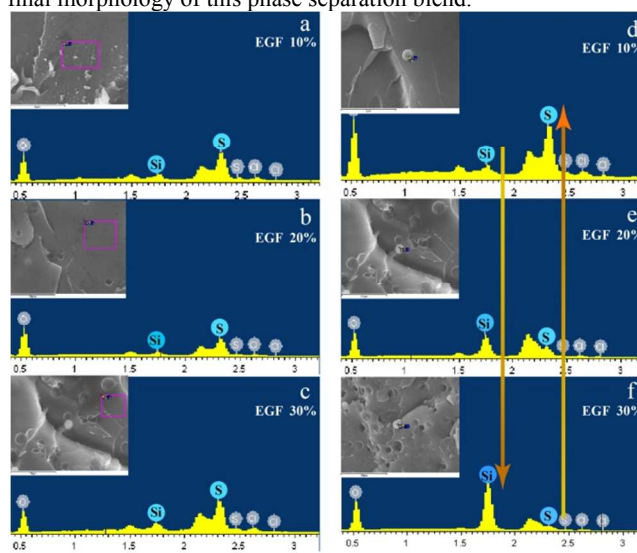
Fig. 5 SEM micrographs and EDS spectra of the epoxy matrix (left) and dispersed particles (right)

Table 1 Abundance of element S and Si in continuous matrix and dispersed particles

Sample	Matrix		Particle	
	S (%)	Si (%)	S (%)	Si (%)
E51	2.31	-	-	-
$F_{0.1}E_{0.9}$	2.30	2.97	2.78	0.57
$F_{0.2}E_{0.8}$	2.32	2.35	0.81	2.92
$F_{0.3}E_{0.7}$	2.35	2.32	0.66	4.88

[a] Footnote text.

Thermoproperties of cured epoxy resins

After curing in a DSC cell up to 300 °C, each sample was allowed to cool down to room temperature and subjected to a second run. From the DSC trace, obtained in the second run, the T_g was determined. The T_g of neat epoxy E51 cured with DDS is 218.9

°C, and as expected, modified silicone epoxy has lower *T*g since the silicone blocks increases the flexibility of the system. The depression of the *T*g of modified epoxy resin indicates that some amount of silicone blocks dissolved in the epoxy system. Despite
5 silicone blocks aggregated as micelles with an increase in the concentration of added EGF, the addition of EGF resin reduces the *T*g of the cured EGF/E51 blends in a linear fashion. Our observations agree with previous work on similar networks[7, 8] .
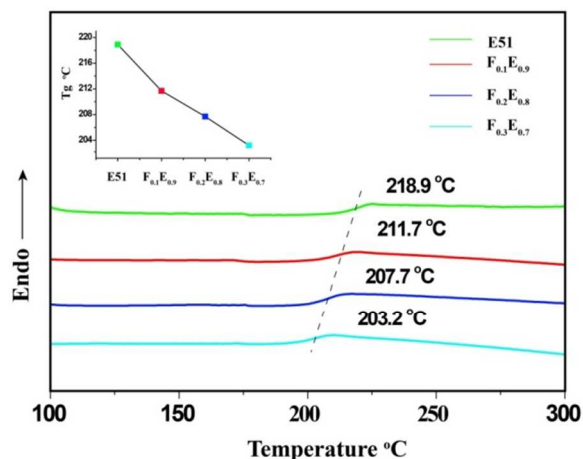
10 **Fig. 6** Glass transition of the cured EGF/E51 blends and the neat epoxy network. The insert is Tg of cured resins
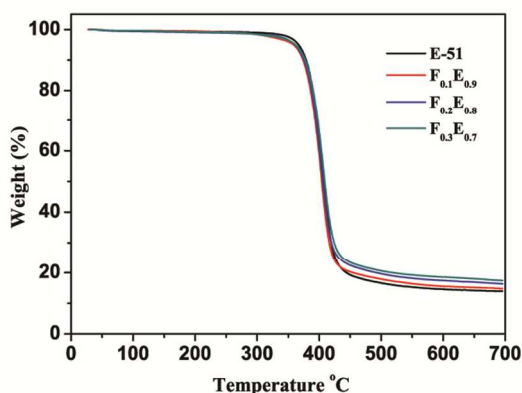
Fig. 7 TGA curves of cured EGF/E51 blends and the neat epoxy network

The thermal stability and the degradation behavior of the cured
15 systems were investigated by thermogravimetric analysis (TGA) under nitrogen atmospheres. The weight loss as a function of temperature and the thermal property parameters for the cured epoxy systems are shown in Fig. 7 and Table 2, respectively. $T_{d,5\%}$ and $T_{d,10\%}$ show that E-51 epoxy resin has slightly higher
20 initial degradation temperature than that of mixed resins. It might be attributed to the higher crosslink density of E-51 resins. As the chain breakage mainly occurs between intermolecular in the beginning of decomposition, the crosslink density plays an important role in deciding the initial decomposition
25 temperature[23]. On the other hand, initial degradation temperature of mixed epoxy resin increases with the increase of EGF content, this should be attributed to rigid diphenyl fluorene and Si-O bond which has better thermostability. Table 2 shows a

higher Yc value of mixed resins comparing with E-51/DDS, and
30 Yc values change regularly with increasing the content of EGF, which could obviously be the contribution of the rigid diphenyl fluorene structure into the crosslink network. In addition, the higher Yc of EGF cured systems are enhanced with respect to the Si-O bond, which has higher bond dissociation and better stability
35 in comparison with C-C and C-O bonds[24-27].
Dynamic mechanical observations were carried out to analyze the dynamic elastic modulus and the occurrence of molecular mobility transitions such as glass transition[28]. Temperature dependence curves of storage modulus (E′) and tan δ values for
40 different cured epoxy systems are presented in Fig.8 and Fig.9 respectively. In the glassy region, the E′ value of cured E51 system was lower than that of modified epoxy. The cured systems

Table 2 Thermal stability parameters for different epoxy/DDS systems

Samples	$T_{d,5\%}$ (°C)	$T_{d,10\%}$ (°C)	T_{max} (°C)	Y_c (%, 600 °C)
$F_{0.3}E_{0.7}$/DDS	361.77	377.58	406.83	18.55
$F_{0.2}E_{0.8}$/DDS	360.78	375.42	402.87	17.42
$F_{0.1}E_{0.9}$/DDS	358.61	374.06	402.67	15.54
E-51/DDS	366.81	378.94	407.60	14.55

$T_{d,5\%}$: temperature of 5% weight loss; $T_{d,10\%}$: temperature of 10% weight
45 loss; T_{max}: temperature of maximum rate of weight loss; Y_c: char yield under nitrogen atmosphere.
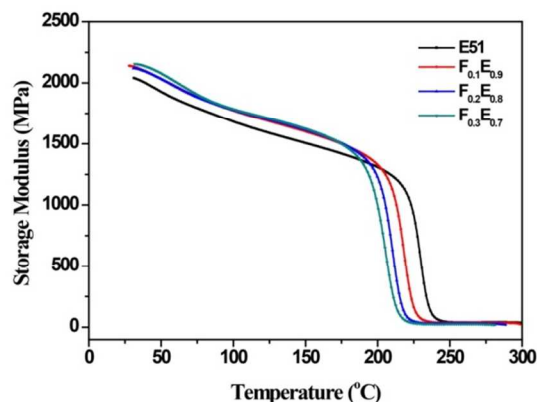
Fig. 8 Storage modulus versus temperature of cured EGF/E51 blends and the neat epoxy network
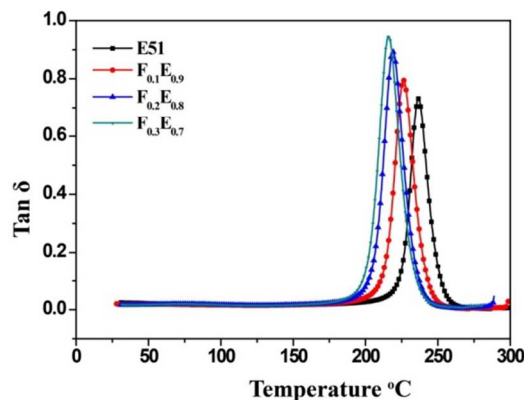
50 **Fig. 9** Tan δ versus temperature of cured EGF/E51 blends and the neat epoxy network

with more content of EGF resins appear to have better retention of E′ value than other cured system. This result might be attributed to the higher rigidity of diphenyl fluorene skeleton in the chain backbone of EGF resin[23]. The diphenyl fluorene based polymer (EGF resin) has a structure in which a bulky fluorene unit protrudes vertically from the polymer main chain. This chemical structure of four phenyl rings connected to a quaternary carbon leads to severe rotational hindrance of the phenyl groups, which in return reduced the rotational mobility of the main chain[29]. However, this situation reversed when it came to the rubbery region. This is consistent with the depression in Tg of the cured resins determined by DSC and DMA. The T_g values (taken as maximum of tan δ curve at 1 Hz) of cured E51, $F_{0.1}E_{0.9}$, $F_{0.2}E_{0.8}$ and $F_{0.3}E_{0.7}$ are 236.6, 226.3, 217.2 and 213.8 ℃ respectively. With more and more inclusion of EGF resin, the peak of tan δ shifts to lower temperature. This may be attributed to the flexibility of silicone blocks. Another reason for the peak shifting could be the decrease in the cross-linking density of the epoxy upon the incorporation of EGF resin[28].

It is well known that absorbed moisture has a detrimental effect on the mechanical properties of epoxy resins, especially at elevated temperature. Therefore, moisture absorption is an important parameter to evaluate whether epoxy resin has high performance or not. Fig.10 showed the moisture uptake of the cured epoxy resins with the varying of time. By comparing the curves of different epoxy/diamine systems, it can be clearly seen that EGF/DDS system had a smaller moisture absorption than that of E-51/DDS system, and with increasing the content of EGF in the mixture resins, the relevant systems presented lower water uptake ability increasingly and took less time to achieve the plateau, which is corresponding to the water uptake at equilibrium. The results above showed that EGF/DDS system possessed a better moisture resistance than that of E-51/DDS system. It was thought that the lower absorbed amount of moisture was attributed to the introduction of silicone and fluorene ring into epoxy. Silicone is known to possess the hydrophobic nature and excellent moisture resistance[30-32]. When Si-O bond was introduced into epoxy, the system would perform a better moisture resistance. During the curing process, hydrophilic hydroxyl groups were generated through the ring opening of epoxy groups[29, 33]. As the average volume of the fluorene skeleton was larger than that of the methyl group in diphenyl A epoxide, it led to a decrease of free volume and
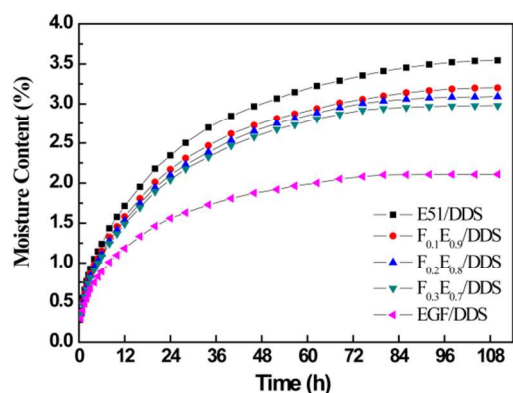
crosslink density in the network of cured systems, which produced less hydroxyl groups and resulted in an improved hydrophobicity of the EGF systems. In addition, EGF had more contents of phenyl group comparing with E-51, thus leading to an increase of nonpolarity of the polymer molecule, which could further depress the moisture absorption[34]. As a result, the EGF/DDS curing system showed significantly lower moisture uptake relative to the E-51/DDS curing system and the incorporation of EGF could effectively improve the moisture resistance of the blend-epoxy curing systems.

4. Conclusions

Amphiphilic silicone epoxy containing diphenyl fluorene was successfully synthesized and used as porogen for cured epoxy resin. The morphology of cured epoxy resin can be easily control by the concentration of amphiphilic silicone epoxy modified by diphenyl fluorene. The compatibility between the EGF and epoxy at low loading (< 10 wt%) was elucidated by SEM image. Higher EGF loading led to obvious phase separation and porous morphology. The migration and aggregation of silicone units was observed by SEM-EDS. Self-assembly induced phase separation establishes a general methodology to prepare porous epoxy monolith.

Acknowledgements

Notes and references

a Key Laboratory of New Processing Technology for Nonferrous Metals and Materials, Ministry of Education, School of Materials Science and Engineering, Guilin University of Technology, 12 Jiangan Road, Guilin 541004, Guangxi, China, e-mail: jwpengd@163.com
b Key Laboratory for Organic Electronics & Information Displays (KLOEID) and Institute of Advanced Materials (IAM), Nanjing University of Posts & Telecommunications (NUPT), 9 Wenyuan Road, Nanjing 210046, Jiangsu, China, e-mail: gutwxdeng@gmail.com

1. Peinemann K.V., Abetz V., and Simon P.F., Nat. Mater., 2007. **6**(12): p. 992-996.
2. Lee, J.H., Wang L.F., Kooi S., Boyce M.C., and Thomas E.L., Nano Lett., 2010. **10**(7): p. 2592-7.
3. Wong K.H., Stenzel M.H., Duvall S., and Ladouceur F., Chem. Mater., 2010. **22**(5): p. 1878-1891.
4. Liu, Y., Lee J.Y., Kang E.T., Wang P., and Tan K.L., React. Funct. Polym., 2001. **47**(3): p. 201-213.
5. Drzal P.L., Halasa A., and Kofinas P., Polymer, 2000. **41**(12): p. 4671-4677.
6. Ng, Y.H. and Hong L., J. Appl. Polym. Sci., 2006. **102**(2): p. 1202-1212.
7. Meng F., Xu Z., and Zheng S., Macromolecules, 2008. **41**(4): p. 1411-1420.
8. Meng F., Zheng S., Li H., Liang Q., and Liu T., Macromolecules, 2006. **39**(15): p. 5072-5080.
9. Wang M.H., Yu Y.F., Wu X.G., and Li S.J., Polymer, 2004. **45**(4): p. 1253-1259.
10. Yu Y.F., Wang M.H., Gan W.J., Tao Q.S., and Li S.J., J. Phys. Chem. B, 2004. **108**(20): p. 6208-6215.
11. Lee H., and Neville K., *Handbook of epoxy resins*. McGraw-Hill: New York, 1967.

Fig. 10 Moisture absorption curves of different epoxy/DDS systems

12. Lubin G., *Handbook of composites*. Nostrand Reinhold: New York, 1982.

13. Chen P. and Wang D.Z. , *Applications of epoxy resins*. Academic: Beijing, 2001.

14. Khurana P., Aggarwal S., Narula A.K., and Choudhary V., Polym. Int., 2003. **52**(6): p. 908-917.

15. Sharmin E., Imo L., Ashraf S.M., and Ahmad S., Prog. Org. Coat., 2004. **50**(1): p. 47-54.

16. Kiefer J., Hilborn J.G., Manson J.A.E., and Leterrier Y., Macromolecules, 1996. **29**(11): p. 4158-4160.

17. Loera A.G., Cava F., Dumon M., and Pascault J.P., Macromolecules, 2002. **35**(16): p. 6291-6297.

18. Guo Q.P., Habrard A., Park Y., Halley P.J., and Simon G.P., J. Polym. Sci., Part B: Polym. Phys., 2006. **44**(6): p. 889-899.

19. Pramanik M., Mendon S.K., and Rawlins J.W., Polym. Test., 2012. **31**(5): p. 716-721.

20. Lin H.C., Chiang J.C., and Wang C.S., J. Appl. Polym. Sci., 2003. **88**(11): p. 2607-2613.

21. Lady J.H., Bower G.M., Adams R.E., and Byrne F.P., Anal. Chem., 1959. **31**(6): p. 1100-1102.

22. Thomas R., Boudenne A., Ibos L., Candau Y., and Thomas S., J. Appl. Polym. Sci., 2010. **116**(6): p. 3232-3241.

23. Dai Z., Li Y., Yang S., Zhao N., Zhang X., and Xu J., Eur. Polym. J., 2009. **45**(7): p. 1941-1948.

24. Pauling L., *The nature of the chemical bond*. New York: Cornell University Press,*3rd.* 1960, Ithica.

25. Sung P.H. and Lin C.Y., Eur. Polym. J., 1997. **33**(6): p. 903-906.

26. Homrighausen C.L. and Keller T.M., Polymer, 2002. **43**(9): p. 2619-2623.

27. Spontón, M., Estenoz D., Lligadas G., Ronda C., Galià *M.*, and Cádiz V., J. Appl. Polym. Sci., 2012. **126**(4): p. 1369-1376.

28. Lee, J.Y., Jang J., Hwang S.S., Hong S.M., and Kim K.U., Polymer, 1998. **39**(24): p. 6121-6126.

29. Kazama S. and Sakashita M., J. Membrane Sci., 2004. **243**(1–2): p. 59-68.

30. Cabanelas J.C., Prolongo S.G., Serrano B., Bravo J., and Baselga J., J. Mater. Process. Tech., 2003.**143-144**: p. 311-315.

31. Lauter U., Kantor S.W., Schmidt-Rohr K., and Macknight W.J., Macromolecules, 1999. **32**(10): p. 3426-3431.

32. Chojnowski J., Cypryk M., Fortuniak W., Ścibiorek M., and Rózga-Wijaset K., Macromolecules, 2003. **36**(11): p. 3890-3897.

33. Swier S., Van Assche G., Vuchelen W., and Mele B.V., Macromolecules, 2005. **38**(6): p. 2281-2288.

34. Xu K., Chen M.C., Zhang K., and Hu J.W., Polymer, 2004. **45**(4): p. 1133-1140.

RSC Advances Accepted Manuscript